Bioelectrochemistry 151 (2023) 108400

Contents lists available at ScienceDirect

Bioelectrochemistry

journal homepage: www.journals.elsevier.com/bioelectrochemistry

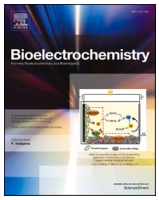

Evaluating the antioxidant activity of secondary metabolites of endophytic fungi from *Hypericum perforatum* L. by an electrochemical biosensor based on AuNPs/AC@CS composite

Bolu Sun [a,1,*], Yanmei Yang [a,1], Yanlei Sun [b,1], Dan Wu [a,1], Lei Kan [a], Chengyang Gao [a], Hongxia Shi [c], Chunyan Sang [d], Tiankun Zhao [a], Lin Yang [a,*], Quhuan Ma [e], Xiaofeng Shi [e,*]

[a] School of Life Science and Engineering, Wenzhou Engineering Institute of Pump & Valve, Lanzhou University of Technology, Lanzhou 730050, Gansu, China
[b] Department of Endocrinology, Wuhan Third Hospital, 430000, China
[c] Lanzhou Zhongjianke Testing Technology Co., Ltd, Lanzhou 730000, Gansu, China
[d] CAS Key Laboratory of Chemistry of Northwestern Plant Resources and Key Laboratory for Natural Medicine of Gansu Province, Lanzhou Institute of Chemical Physics, Chinese Academy of Sciences (CAS), Lanzhou 730000, China
[e] Gansu Academy of Medical Science, Lanzhou 730050, Gansu, China

ARTICLE INFO

Keywords:
Hypericum perforatum L. (*HP* L.)
Secondary metabolites of endophytic fungi (SMEF)
Electrochemical biosensor
Evaluation of antioxidant activity

ABSTRACT

Due to the variety and activity of secondary metabolites of endophytic fungi (SMEF) from medicinal plants, and the operation cumbersome of existing methods for evaluating the activity, there is urgent to establish a simple, efficient and sensitive evaluation and screening technology. In this study, the prepared chitosan functionalized activated carbon (AC@CS) composite as the electrode substrate material was used to modify glassy carbon electrode (GCE), and the gold nanoparticles (AuNPs) was deposited on AC@CS/GCE by cyclic voltammetry (CV). A ds-DNA/AuNPs/AC@CS/GCE electrochemical biosensor for evaluating the antioxidant activity of SMEF from *Hypericum perforatum* L. (*HP* L.) was fabricated using the method of layer by layer assembly. The experimental conditions affecting the evaluation results of the biosensor were optimized by square wave voltammetry (SWV) using $Ru(NH_3)_6^{3+}$ as the probe, and the antioxidant activity of various SMEF from *HP* L. was evaluated by the proposed biosensor. Meanwhile, the results of the biosensor were also verified by UV–vis. According to the optimized experimental results, the biosensors had a high levels of oxidative DNA damage at pH 6.0 and Fenton solution system with Fe^{2+} to OH^- ratio of 1:3 for 30 min. Among the crude extracts of SMEF from roots, stems and leaves of *HP* L., the crude extracts from stems presents a high antioxidant activity, but it was weaker than L-ascorbic acid. This result was consistent with the evaluation results of UV–vis spectrophotometric method, also the fabricated biosensor presents high stability and sensitivity. This study not only provides a novel, convenient and efficient way for rapid evaluating the antioxidant activity of a wide variety of SMEF from *HP* L., but also provides a novel evaluation strategy for the SMEF from medicinal plants.

1. Introduction

Hypericum perforatum L. (*HP* L.) is a perennial herb mainly distributed in Gansu, Shaanxi, and Xinjiang of China, with a long medical history [1]. It was first recorded in the "Supplement to Compendium of Materia Medica", as well in "Nanjing folk herbs" and "Records of Sichuan Traditional Chinese Medicine" [2], which has a history of more than 2,000 years. Its efficacy is mainly reflected in analgesic, anti-inflammatory, astringent and hemostatic aspects [3]. Modern pharmacological studies show that it has antioxidant [4], antidepressant [5], anticancer [6], and antibacterial [7] effects. Because of its unique pharmacological effects, *HP* L. has a good prospect of research and development. However, with the continuous research on *HP* L., its market demand is gradually increasing, and a shortage of the market is slowly appearing. Therefore, it is important to find effective substitutes for *HP* L., on the one hand it can meet the increasing market demand of *HP* L. On the other hand, it can open up new paths for the development and utilization of *HP* L. with high medicinal value.

* Corresponding authors.
E-mail addresses: sunbl14@lzu.edu.cn (B. Sun), Yanglin-401@163.com (L. Yang), shixiaofeng2005@sina.com (X. Shi).
[1] These authors contributed equally to this work.

https://doi.org/10.1016/j.bioelechem.2023.108400
Received 12 September 2022; Received in revised form 5 January 2023; Accepted 12 February 2023
Available online 15 February 2023

Endophytic fungi from medicinal plants, as a symbiotic group of plants, can metabolize and produce a variety of bioactive substances [8]. In recent years, it had received increasing attention and application, especially in the field of endophytic fungal microbial pharmaceuticals based on medicinal plants, such as the production and preparation of antibiotics, anticancer drugs, antibacterial drugs, antidiabetic drugs, antioxidants, etc. [9] Wu et al. [10] studied the endophytic fungi community structure from the medicinal plant Dithistle and their potential to provide antimicrobial secondary metabolites. The results showed that among the isolated endophytic fungi, the ethyl acetate extract of Penicillium sp.st DIF9 had stronger antimicrobial activity. Hasan et al. [11] isolated the endophytic fungi from cherimoya leaves and tested the inhibitory effect of the extract against yeast, cervical cancer cells and normal cells by MTT assay. The results indicated that the crude extract of Sir-SM2 endophytic fungus was highly cytotoxic to cervical cancer cells (HeLa cells) and less harmful to normal cells. Therefore, the strategy from medicinal plant endophytic fungal research can be used to find secondary metabolites to replace the natural active ingredients in *HP* L., and it provides technical support for the conservation of *HP* L. plant resources and further promotes high-quality and in-depth development and application of *HP* L.

Medicinal plant endophytic fungi [12] are a huge system and specific fungal groups which can produce abundant secondary metabolites with a variety of activities (e.g. antitumor, antibacterial, antioxidant, insecticidal, etc.), and it is an important source for the search of novel drugs. Among them, antioxidant activity [13] as a hot research aspect in recent years, plays an antioxidant role by providing electrons to free radicals before they oxidize other cellular components. At present, it had been intensively studied and applied in the fields of anti-aging and cancer. Therefore, the screening of substances with antioxidant activity from SMEF in medicinal plants for disease prevention and treatment has become an important direction in the current research and development of new drugs. However, the main methods used for the evaluation of antioxidant activity of endophytic fungi are oxygen radical absorbance capacity (ORAC) [14], total radical trapping antioxidant capacity parameter (TRAP) [15], 1,1-diphenyl-2-picrylhydrazyl method (DPPH) [16], copper (II) reduction capacity assay [17], etc. But, the endophytic fungi isolated are characterized by many kinds and samples, their activity evaluation is time-consuming and tedious. Therefore, a sensitive, rapid, inexpensive and efficient evaluation method is urgently needed.

Electrochemical biosensors [18] have been extensively studied in the field of evaluating the antioxidant activity because of their high sensitivity, good stability, simple operation, and low cost. Ye et al. [19] used CNFs-doped photosensitive hydrogels to construct a cellular 3D culture system and constructed cellular electrochemical biosensors based on MnO_2NWs and AuNPs-modified GCEs. The biosensor successfully evaluated and graded the antioxidant activity of 16 anthocyanins and their glycoside derivatives. Liu et al. [20] constructed a novel $O_2^{\bullet-}$ electrochemical sensor using AgNPs-MC modified glassy carbon electrode for investigating the enhancing cellular antioxidant defense system, which exhibited high catalytic capacity and also successfully used to detect the release of O_2 from living cells. Hence, electrochemical biosensors have unique advantages in the evaluation of antioxidant activity. Among the electrochemical evaluation methods, DNA electrochemical biosensors [21] are widely used for the evaluation of antioxidant activity due to their rapid response and good sensitivity. In the process of application, ds-DNA fixed on the electrode surface was attacked by ·OH in Fenton solution, which led to the breakage of ds-DNA and the release of bases, thus causing DNA damage. However, antioxidants were added to Fenton solution can effectively remove ·OH and reduced the amount of DNA damage [22]. Therefore, the antioxidant activity of SMEF from *HP* L. can be evaluated by electrochemical detection of DNA damage.

However, the analytical performance of the activity evaluation biosensor is often affected by the choice of the substrate electrode and the performance of the electrode modification material. Activated carbon (AC) has received a lot of attention from researchers because of its huge specific surface area, high pore density, low cost, and incomparable good mechanical and chemical stability compared with other alternatives. Aysun et al. [23] constructed an electrochemical sensor for the determination of glucose in real serum using AC as a modification material to enhance the electrical conductivity. Chitosan (CS) [24] was used as a stabilizer with film-forming and contamination resistance, and it combined with AC to provide high electrical conductivity and adsorption capacity. Lota et al. [25] combined AC and CS as materials for modifying electrodes, which showed that AC coated by CS exhibited good charge propagation and excellent cycling stability. Gold nanoparticles (AuNPs) are often used as the main material for the construction of electrochemical sensors due to their biocompatibility and good electronic properties [26]. Tang et al. [27] successfully constructed electrochemical sensors for the determination of antioxidant activity of lignocaine based on electrodeposited graphene quantum dots and gold nanoparticles. The sensors prepared under optimized conditions showed a large electrochemical active surface area, good electrocatalytic activity and stability. It can be seen that AC and CS as well as AuNPs have great advantages in improving the performance of proposed sensors.

Based on this, a ds-DNA/AuNPs/AC@CS/GCE electrochemical biosensor had been fabricated for the evaluation of antioxidant activity of SMEF from *HP* L. which was constructed by electrodeposition of AuNPs on the electrodes modified by activated carbon functionalized with chitosan (AC@CS). Then the ds-DNA was firmly immobilized on the surface of AuNPs/AC@CS/GCE with the help of the adsorption of AC and CS and the biocompatibility of AuNPs. After Fenton's solution damaged the ds-DNA/AuNPs/AC@CS/GCE electrode, the DNA film on the electrode surface was damaged, and the electrochemical signals detected in $Ru(NH_3)_6^{3+}$ probe solution were different from those before the damage [28]. The antioxidant activity can be evaluated through the difference of the detected electrical signals. Therefore, using $Ru(NH_3)_6^{3+}$ as the probe solution, the Fenton solution damage to DNA and the inhibition of free radical damage to DNA by different SMEF from *HP* L. were investigated by square wave voltammetry (SWV) (Scheme 1). The evaluation results of the biosensor were also verified by UV–vis. It hopes to provide a means for rapid, accurate and efficient evaluation of antioxidant activities of SMEF from *HP* L., and also provides a novel evaluation strategy for rapid screening of SMEF from medicinal plants.

2. Experimental

2.1. Apparatus

CHI660E electrochemical workstation consists of a conventional three-electrode system. The working electrode is a bare glassy carbon electrode or a modified glassy carbon electrode (GCE), and the saturated glycerol electrode and platinum wire electrode are the reference and auxiliary electrodes (Shanghai Chenhua Instrument). SB-5200DTD Ultrasonic cleaner (Ningbo Xinzhi Biological Technology). Rotary evaporator RE-52A (Shanghai Bilang Instrument). SW-CJ-1D (practical vertical novelty). Single clean bench (Shanghai Sujing Industrial). Electric thermostat incubator (Shanghai Yuejin Medical Equipment). Thermostatic oscillator (Changzhou Guohua Electric). 722N visible spectrophotometer (Shanghai Youke Instrument).

2.2. Chemicals and reagents

Herring sperm DNA (ds-DNA), $HAuCl_4$ (Tianjin Comio Chemical Reagent). Chitosan (CS) (Sarn Chemical Technology). Activated carbon (AC) (Nanjing Xianfeng Nanomaterials Technology). Through-leaf *Hypericum perforatum* L. (Harvested from Shanmen Town, Qingshui County, Tianshui City, Gansu Province, China). $Ru(NH_3)_6Cl_3$ (98 %, Sarn Chemical Technology (Shanghai)). L-ascorbic acid (AA), Fenton solution, methylene blue (MB) (Tianjin Kaixin Chemical Industry). Potassium ferricyanide (Tianjin Baishi Chemical). All reagents used in this experiment were analytically pure.

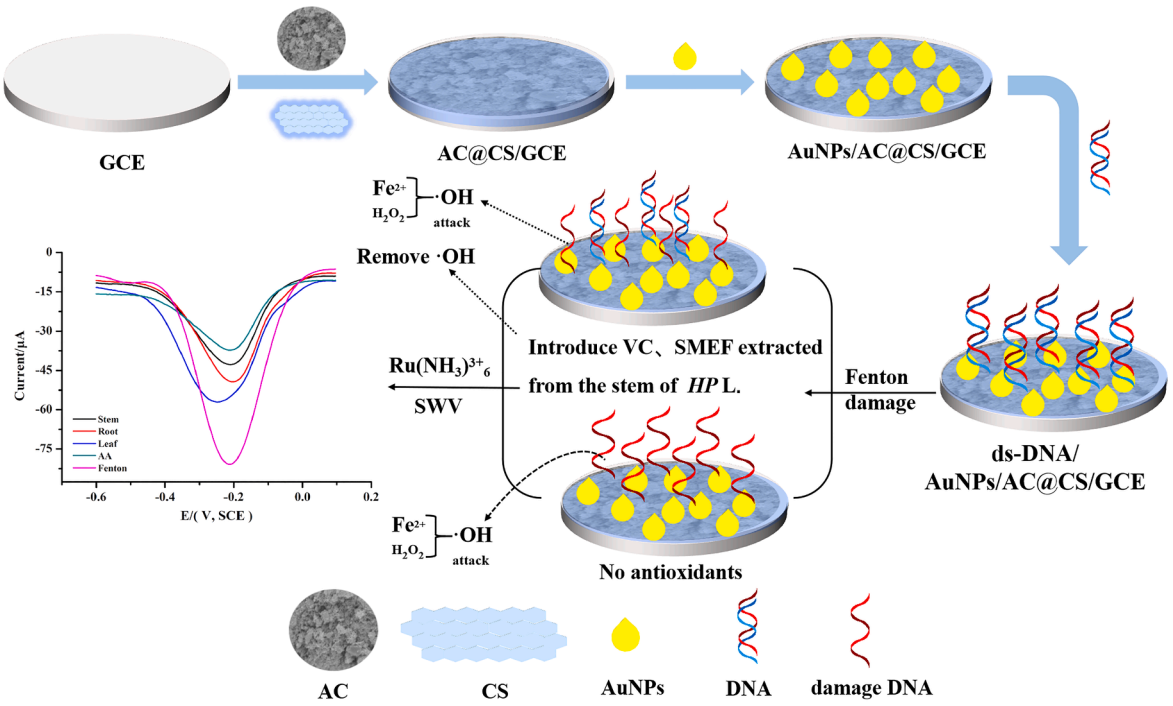

Scheme 1. Schematic representation of constructing ds-DNA/AuNPs/AC@CS/GCE electrochemical biosensor for evaluating the antioxidant activity of SMEF from *HP* L.

2.3. Preparation of crude extracts of SMEF from HP L.

2.3.1. Isolation, purification and preservation of endophytic fungi

The roots, stems and leaves of the picked *HP* L. [29,30] were washed, and then cut into small pieces with sterilized blades by tissue cutting method. After soaking in 75 % ethanol (C_2H_5OH) and sodium hypochlorite (NaClO) for 30 s and 3 min, respectively, and then rinsed with sterile water three times, and the excess water was blotted out with sterile filter paper. It was advisable to cut the small sections to 2–3 pieces per dish, picked with sterile forceps, and inoculate on Potato Dextrose Agar (PDA) medium. And the culture medium was placed in a constant temperature incubator at 28 ℃ for 3–5 days. After mycelia grew around the cut block, the inoculum ring was used to pick the bacteria and inoculate them on the new PDA medium until they grew, and the operation was repeated until a single colony was obtained. The above operations were performed in the ultra-clean table. Finally, the obtained strains were numbered, and the strains were preserved with inclined plane and glycerol for the convenience of subsequent experiments.

2.3.2. Morphological observation and preliminary identification of endophytic fungi

All the isolated strains were incubated in the newly prepared isolation medium at 28 ℃. The colony characteristics were recorded, including colony morphology, mycelium length, colony color, colony edge morphology and growth rate, etc. After that, the endophytic fungi in the roots, stems and leaves from *HP* L. were initially identified.

2.3.3. Preparation of crude extracts of SMEF

In the clean workbench, the mycelium grown from the purified mycelium was selected and inoculated into 300.0 mL Potato Dextrose Broth (PDB) medium by inoculating ring, and shaken for 15 days in a 180 RPM shaker at 28 ℃. The fermentation products were filtered with a cloth funnel to obtain mycelium and bacterial broth respectively. Then the mycelium was extracted three times with equal volume of ethyl acetate solvent, and the solvent was recovered by combining the extracts to obtain the ethyl acetate extract. After drying at 50 ℃ and grinding, the mycelium was placed in a 500.0 mL round-bottom flask for reflux extraction with methanol solvent in water bath. The above steps were repeated three times, the extract was combined, and the solvent was recovered. Finally, methanol extract of mycelium was obtained. Ethyl acetate extract of fermentation broth and methanolic extract of mycelium were stored in a refrigerator at 3 ℃ and set aside. The sample weights of ethyl acetate extract of fermentation broth and methanolic extract of mycelium obtained from the root, stem and leaf parts were weighed accurately and recorded. Dissolving thoroughly with an appropriate amount of absolute ethanol organic solvent. If necessary, the samples were dissolved with the assistance of ultrasound. The sample solution concentration was calculated to ensure subsequent determination of the electrochemical response.

2.4. Preparation of AC@CS composite

20.00 mg CS was added to 100.0 mL of 1 % acetic acid solution and stirred continuously until no bubbles which were generated to obtain clear and transparent CS solution. The prepared CS solution was stored at 3 % for using. 10.00 mg AC was added to 10.0 mL distilled water, and the AC suspension was evenly dispersed by ultrasound for 2 h. Then 5.0 mL AC suspension was added to 10.0 mL CS solution and dispersed by ultrasound for 30 min to make AC evenly dispersed in CS solution.

2.5. Preparation of ds-DNA/AuNPs/AC@CS/GCE-modified electrode

The bare GCE was polished to a mirror surface with 0.30 and 0.05 μm alumina powder sequentially on a chamois. Then the electrodes were washed successively with methanol and distilled water for 10 min in an ultrasonic bath and dried in air. The GCE modified by AC@CS was obtained through carefully dripping 20 μL of the composite solution onto the GCE, and drying under an infrared lamp. After drying, the modified electrode AC@CS/GCE was placed in 10.0 mL 0.10 mol/L H_2SO_4 solution containing 1.00 mM $HAuCl_4$. AuNPs were deposited by cyclic voltammetry (CV) at a rate of 50 mV/s in the potential range of −0.8 to 1.2 V, and AuNPs/AC@CS/GCE was obtained. Finally, 10 μL of 0.50 mg/mL ds-DNA was applied dropwise on the AuNPs/AC@CS/GCE modified electrode, drying it naturally at 3 ℃ and DNA was washed off the

electrode surface with PBS buffer solution pH 7.0. The modified electrode was ds-DNA/AuNPs/AC@CS/GCE.

2.6. Detection of ds-DNA damage process

By referring to the method of Kaya et al. [31], the process of DNA damage was examined. Firstly, the ds-DNA/AuNPs/AC@CS/GCE modified electrode was placed in 1.00 mmol/LRu$(NH_3)_6^{3+}$ (containing 50.00 mmol/L KCl) probe solution, and the electrochemical response signal before damage was obtained by square wave voltammetry (SWV) scanning. The ds-DNA/AuNPs/AC@CS/GCE electrode before the damage detection was polished and modified to prepare the ds-DNA/AuNPs/AC@CS/GCE modified electrode again. which was first incubated in 20.0 mL Fenton solution (PBS solution, pH 7.0, containing 1.00 mmol/L $FeSO_3$ and 5.00 mmol/L H_2O_2) at room temperature for 30 min, and washed with pH 7.0 PBS buffer solution. After washing, electrode was placed in Ru(NH_3)3 + 6probe solution for SWV scanning, and the electrochemical response signal after damage was obtained. Similarly, the re-polished ds-DNA/AuNPs/AC@CS/GCE electrode was put into Fenton solution containing antioxidants and incubated for 30 min at room temperature (antioxidant: L-ascorbic acid, 0.90 mg/mL). The electrode was taken out and washed with PBS solution pH 7.0, and then placed in $Ru(NH_3)_6^{3+}$ solutions for SWV scanning to detect the inhibition of DNA damage. (To avoid the error of the experiment, the same electrode was used during the experiment).

2.7. Detection of antioxidant activity of crude extracts of SMEF from HP L.

The DNA damage assay in 2.6 was repeated. On this basis, the modified ds-DNA/AuNPs/AC@CS/GCE electrodes were incubated in Fenton solution containing L-ascorbic acid (AA), ethyl acetate extract of fermentation broth of roots, stems and leaves from *HP* L. and methanolic extract of mycelium (both at 0.90 mg/mL) for 30 min at room temperature. The damaged electrode in Fenton solution was washed with PBS solution pH 7.0, and the electrode was placed in $Ru(NH_3)_6^{3+}$ solution for SWV scanning (each time, the electrode was polished and modified again).

2.8. Evaluation of antioxidant activity by UV–vis

Using methylene blue (MB) as indicator, UV–vis [32,33] was used to detect the absorbance of ds-DNA after treatment in different solutions. The absorbance ratio (A_t/A_0) was used to measure the degree of ds-DNA damage within the membrane and the antioxidant properties of the SMEF from *HP* L. and AA. Firstly, 10 μL of 0.10 mg/mL ds-DNA solution was added to 20.0 mL of Fenton solution and Fenton solution containing the antioxidant AA and SMEF from *HP* L. for 0 min, 10 min, 20 min, 30 min and 40 min, respectively. The ds-DNA solutions treated for different times were added to the prepared 20.00 μmol/L MB (containing 0.10 mol/L PBS) solution, absorbance was detected at 400 nm–750 nm. While the absorbance of MB without ds-DNA solution was measured and the results were used as a control. (A_t was the absorbance value of methylene blue (MB) at t min of damage in the Fenton system containing the antioxidant AA and the SMEF from *HP* L. A_0 was the absorbance value of MB at 0 min of damage in the Fenton system).

3. Results and discussion

3.1. Isolation and purification of endophytic fungi from HP L.

A total of 10 endophytic fungi were isolated in this thesis and transferred to newly prepared slant medium in turn. Then the endophytic fungi were incubated at 28 ℃ for 3–5 days and stored in a refrigerator at 3 ℃. The numbers of isolated endophytic fungi from *HP* L. are shown in Table S1. The colony morphology of the 10 strains of endophytic fungi was different, and the mycelium morphology was also very different. As shown in Fig. S1 and Table S2, the results showed that the colonies were mainly green, dark green, white, pink, black and so on. The mycelium morphology mainly includes tufted, plush, etc. The edges of some colonies climb the wall, and some have neat edges. At the same time, the surface of the colony, some with a certain amount of water, some relatively dry.

3.2. Fermentation of endophytic fungi and preparation of crude extracts of secondary metabolites to be tested

The ethyl acetate extract of the fermentation broth and the methanol extract of the mycelium obtained from the root, stem and leaves of *HP* L. which were weighed. The sample net weight was obtained and recorded. The recording results were shown in Table S3, after the crude extract of the secondary metabolites of the strain was fully dissolved with an appropriate amount of anhydrous ethanol, the concentration of the sample solution was calculated. The prepared solution was applied dropwise to the surface of the modified electrode with a pipette gun to facilitate the subsequent corresponding electrochemical detection.

3.3. Preparation and morphological characterization of the modified electrode

Fig. 1 A showed Fourier transform infrared spectroscopy (FTIR) of AC, CS and AC@CS. At 3442 cm^{-1}, CS had an absorption peak of O—H stretching vibration and the —NH stretching vibration absorption peak overlapping and widening. The peak value of 2865 cm^{-1} was obtained from the stretching vibration of C—H. At 1630 cm^{-1} was the characteristic peak caused by amino deformation. The vibration absorption peak with symmetric deformation from C—H appears at 1369 cm^{-1}. The peak values of 2346 cm^{-1}, 1579 cm^{-1},1189 cm^{-1} in AC were caused by C—O stretching vibration, C═O stretching vibration in lactone and alkyne group, respectively. The AC@CS infrared spectrum basically contains the important characteristic peaks of AC and CS, which indicated the successful combination of AC and CS.

Raman was used to characterize the materials of AC and AC@CS. The results were shown in Fig. 1 B, the corresponding characteristic peaks of AC and AC@CS electrode materials were about 1350 cm^{-1} and 1600 cm^{-1}, respectively, which corresponded to the D characteristic peaks and G characteristic peaks of typical graphite-like materials. The D band of AC was hybridized carbon atoms by SP_3, and the G band was hybridized carbon atoms by SP_2. The characteristic peak at 1600 cm^{-1} belonged to the characteristic band of CS. Raman spectrum represents the successful recombination of CS and AC, and the result was the same as the FTIR spectrum result.

As shown in Fig. 1 C, the surface of the composite AuNPs/AC@CS modified electrode was obviously concave and convex with the presence of fine particles, and the rough edges around the particles were relatively stiff. The bright spot indicated the successful adhesion of gold nanoparticles. In Fig. 1 D, when ds-DNA was applied to the modified electrode surface, ds-DNA was bound to the composite AuNPs/AC@CS modified electrode surface by electrostatic interaction and physical adsorption. It showed uneven morphology, small particles appear agglomeration phenomenon, and the whole particle was relatively smooth around. As shown in Fig. 1 E, the ds-DNA/AuNPs/AC@CS/GCE electrode surface showed an undulating and rougher morphology after 30 min of damage by Fenton solution. The reason may be caused by the chain breakage of ds-DNA chains and base oxidative damage of ds-DNA chain affected by Fenton solution. There was also the possibility of Fe^{2+} forming complexes with ds-DNA.

3.4. Preparation and optimization of modified electrode

The process characteristics of the DNA electrochemical sensor preparation were investigated by cyclic voltammetry (CV) and

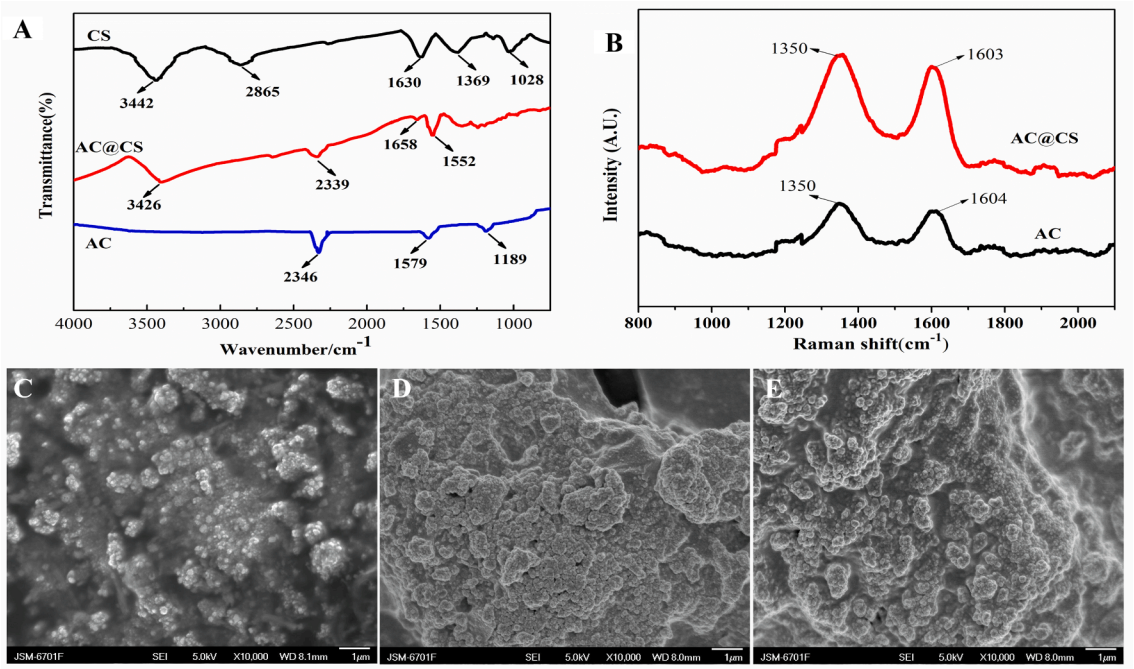

Fig. 1. (A) FTIR spectra of AC, CS, AC@CS. (B) Raman spectra of AC, CS, AC@CS. SEM images of (C) AuNPs/AC@CS/GCE, (D) ds-DNA/AuNPs/AC@CS/GCE, and (E) ds-DNA/AuNPs/AC@CS/GCE after 30 min of Fenton's reagent action.

electrochemical impedance spectroscopy (EIS). As shown in Fig. 2 A, only a pair of very weak redox peaks existed at the bare electrode (curve a), and after modification of the AC@CS composite (curve b) led to a significant increase in the redox peak current value, which continued to increase after further deposition of AuNPs (curve c). This was probably the AuNPs/AC@CS material increased the effective surface area of the electrode and promoted the electron transfer rate of the electrochemical reaction. When DNA was immobilized on the AuNPs/AC@CS surface (curve d), the redox peak $[Fe(CN)_6]^{3-/4-}$ obviously started to decrease, which was due to the fact that the film formed by ds-DNA hindered electron transfer on the electrode surface, making the electrochemical response signal significantly reduced. When the ds-DNA/AuNPs/AC@CS/GCE was damaged by Fenton system, the redox results obtained by CV scanning method continued to decrease. That was due to the double-stranded structure of DNA is likely to have been destroyed after DNA damage.

Thus, the conformation of DNA was changed and furthered hinders the electron transfer on the electrode, resulting in a continuous decrease of the response signal.

Fig. 2 B showed that the Nyquist curves of the modified electrode in 3 mmol/L $[Fe(CN)_6]^{3-/4-}$ solution. The resistance of the bare electrode (curve a) was significantly greater than that of the modified electrode. When the AC@CS composite was modified (curve b), the resistance of the electrode decreased significantly. It was due to the excellent conductivity of AC@CS accelerating the electron transfer rate on the surface of the electrode. After further deposition of AuNPs (curve c), the resistance of the electrode reached the minimum value. This was because the AuNPs coating made the modified electrode obtain a smaller diameter and the electron transfer rate was significantly improved. When the electrode was modified with ds-DNA (curve d), the charge transfer resistance increased significantly because the formed DNA membrane impedes the transfer of electrons. After the ds-DNA/AuNPs/AC@CS/GCE modified electrode was damaged by the Fenton system, the resistance value continued to increase (curve e). It may be the generation of ·OH, which led to a series of conformational were changed in DNA after damage, including double strand break, base dissociation, thus promoting the electron transfer rate on the electrode surface.

$Ru(NH_3)_6^{3+}$ is an electrochemical probe that can provide sensitive detection of ds-DNA damage. In this experiment, 1.00 mmol/L Ru $(NH_3)_6^{3+}$ was used as a probe to detect intact and damaged ds-DNA processes by the SWV method. And the damage to DNA was evaluated by comparing the relative peak current ratio (I_{pt}/I_{p0} [34], I_{pt} is the peak current value detected at different time of damage. I_{p0} is the peak current value detected at 0 min of damage). As shown in Fig. 2 C, the trend of I_{pt}/I_{p0} of ds-DNA/AuNPs/AC@CS/GCE modified electrode immersed in different system solutions for different times, respectively. It can be seen from the figure that when the ds-DNA/AuNPs/AC@CS/GCE modified electrode was in Fenton solution (curve d), I_{pt}/I_{p0} reached a maximum value of about 1.68 times after 30 min of damage to ds-DNA. However, in the other three single-component solutions, including H_2O_2 solution (curve a), Fe^{2+} solution (curve c), and PBS buffered solution with pH 6.0 (curve b), I_{pt}/I_{p0} did not change significantly. Additionally, when only PBS and Fe^{2+} existed, the curves were relatively flat and it basically did not change significantly. The above results indicate that ·OH produced by Fenton solution caused certain damage to DNA thin film on ds-DNA/AuNPs/AC@CS/GCE electrode. However, the double-strand broke and based exposure after DNA damage which will trigger the following reactions, and causing the current response signal to change. Based on this, the electrochemical determination of DNA damage by the sensor can be achieved.

$$ds-DNA \rightarrow DNA(Guanine)$$

$$Ru(NH_3)_6^{3+} + DNA(Guanine) \rightarrow Ru(NH_3)_6^{2+} + DNA(Guanine^{+})$$

$$Ru(NH_3)_6^{2+} = Ru(NH_3)_6^{3+} + e^{-}$$

The effect of DNA fixation on the ds-DNA/AuNPs/AC@CS/GCE modified electrode was investigated in 4.00 mmol/L $K_3[Fe(CN)_6]$/$K_4[Fe(CN)_6]$ solution containing 0.01 mmol/L KCl. As shown in Fig. 2 D, this current response signal tended to a flat state at the ds-DNA modification amount of 10 μL and beyond. When the fixation amount was less than 10 μL, the current response signal was larger. It was probably due to the incomplete film formation of ds-DNA, which promoted the transfer of electrons on the electrode surface. Therefore, in the subsequent experiments, we chose an immobilization volume of 10 μL for ds-DNA to continue the experiments.

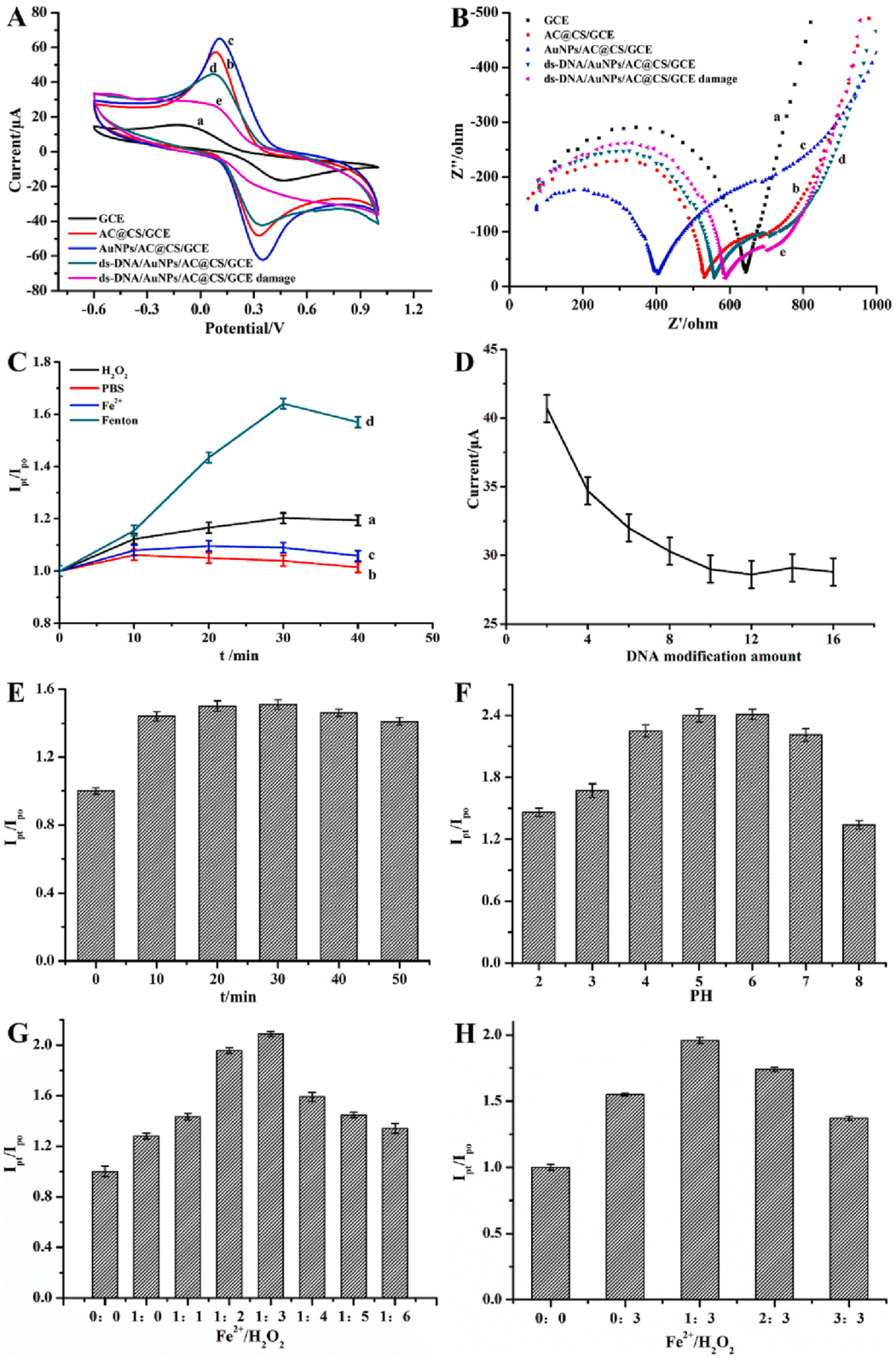

Fig. 2. (A) CV curves and (B) EIS curves of (a) GCE, (b) AC@CS/GCE, (c) AuNPs/AC@CS/GCE, (d) ds-DNA/AuNPs/AC@CS/GCE, (e) ds-DNA/AuNPs/AC@CS/GCE in 3.00 mmol/L $K_3[Fe(CN)_6]/K_4[Fe(CN)_6]$ solution containing 0.01 mmol/L KCl. (C) The linear relationship between oxidation peak current (I_{pt}) and pre-injury peak current (I_{p0}) curves of ds-DNA/AuNPs/AC@CS/GCE in 3.00 mmol/L H_2O_2 (a), pH 6.0 PBS buffer solution (b), 1.00 mmol/L Fe^{2+} (c) and Fenton reagent (d) after different times of damage in $Ru(NH_3)3 + 6$ probe solution by SWV. (D) The influence of ds-DNA fixation amount on ds-DNA damage degree. (E) is a linear bar chart of the ratio of oxidation peak current (I_{pt}) and pre-damage peak current (I_{p0}) measured by SWV during Fenton reagent damage time. (F) is the linear bar chart of the effect of pH value in Fenton solution on the change of I_{pt}/I_{p0} detected by SWV. (G) is the bar chart of I_{pt}/I_{p0} trend detected by SWV when the concentration of fixed Fe^{2+} at 1.00 mmol/L, H_2O_2 concentration is changed and the molar ratio of Fe^{2+} and H_2O_2 changes between 0:0–1:6. (H) is the bar chart of I_{pt}/I_{p0} trend detected by SWV when the concentration of fixed H_2O_2 at 3.00 mmol/L, varying the Fe^{2+} concentration, and changing the molar ratio of Fe^{2+} and H_2O_2 between 0:0 and 3:3.

The effect of immersion in the Fenton system consisting at pH 6.0 PBS solution for 0–50 min on I_{pt}/I_{p0}. Fig. 2 E showed that the value of I_{pt}/I_{p0} reached the maximum after the ds-DNA/AuNPs/AC@CS/GCE modified electrode was damaged by the Fenton system for 30 min, and showed a gradual decrease when the damage time was longer than 30 min. Therefore, 30 min was chosen as the best damage time for subsequent experiments.

The pH of the Fenton solution was chosen to range from 2.0 to 8.0. As shown in Fig. 2 F, with the increase of solution pH value, I_{pt}/I_{p0} firstly increased and then decreased, reaching the maximum at pH 6.0. The results indicated that the ds-DNA/AuNPs/AC@CS/GCE modified electrode was almost completely damaged after 30 min of damage in the Fenton solution damage system at 6.0. Therefore, pH 6.0 was chosen as the optimal pH for the Fenton system in the subsequent experiments.

Fig. 2 G showed the change of SWV response signal when the concentration of Hydrogen peroxide was changed and the concentration of Fe^{2+} was fixed at 1.00 mmol/L. When the molar ratio of Fe^{2+} and H_2O_2 was 1:3, I_{pt}/I_{p0} reached the maximum value. Similarly, as shown Fig. 2 H, when H_2O_2 concentration was fixed at 3.0 mmol/L and Fe^{2+} concentration was changed. When the molar ratio of Fe^{2+} and H_2O_2 was still 1:3, the value of I_{pt}/I_{p0} reached the maximum and the damage degree reached the maximum. Therefore, the molar ratio of Fe^{2+} and H_2O_2 in Fenton system in subsequent experiments is 1:3 (SWV was used to detect the damage time, PH and molar ratio between Fe^{2+} and H_2O_2 of Fenton's solution, as shown in Fig. S2).

3.5. Electrochemical evaluation of antioxidant activity of crude extracts of SMEF from HP L.

Under optimized experimental conditions, the ds-DNA/AuNPs/AC@CS/GCE modified electrode was used to compare the antioxidant activities of AA and crude extracts of SMEF from root, stem and leaf. As shown in Fig. 3 A, 3B and 3C, under the same conditions of AA, ethyl acetate extract of fermentation broth and mycelium methanol extract (all 0.90 mg/mL), the determination results of the electrochemical response signal of the crude extracts of SMEF from the root, stem and leaf were compared. The results showed that, the peak current of root, stem and leaf was smaller than that of mycelium methanol extract. As shown in Fig. 3 D, the response signal of the crude extract of fermentation broth ethyl acetate extract of SMEF from the stem part of *HP* L. was the best in all three parts and the strongest antioxidant activity. Therefore, the ethyl acetate extract from the fermentation broth of the crude extract of SMEF from the stem of *HP* L. was taken as the actual sample in the subsequent experiment. It was denoted as G-S-1.

Compared with I_{pt}/I_{p0} modified electrode damaged by Fenton solution for different times. As shown in Fig. 3 E, 3F, 3 G and 3H, the I_{pt}/I_{p0} of the modified electrode after damage by Fenton solution containing AA and G-S-1 was significantly smaller. And the antioxidant activities of the two substances in the same concentration added to the AA and G-S-1 sample solutions were in the following order. This is because the two enolic hydroxyl groups in the AA molecule are oxidized to dehydrin AA. It can also be reduced to AA by hydrogenation, and this structural interchange made AA have strong antioxidant activity. While G-S-1 had a more complex structure because of its crude extract, and the content of components with antioxidant effect in the whole herb of *HP* L. plant was relatively small, such as the content of flavonoids with very significant antioxidant activity is only 11.7 %. Therefore, the antioxidant activity of G-S-1 is weaker than that of AA. At the same time, the weak antioxidant effect of G-S-1 may be due to the combined effect of tannins, hyperin and quercetin contained in the whole plant itself.

3.6. Stability and reproducibility of the sensor

The relative standard deviation of the SWV of the same DNA electrode measured 10 times in parallel was 2.76 %. The relative standard deviation of the SWV detection of 4 electrodes in the same system was 4.35 %. And the oxidation peak current was 91.7 % of the initial current after 5 days in a refrigerator at 4 ℃. The results showed that, the electrode has good reproducibility and stability.

3.7. Evaluation of antioxidant activity of crude extracts of SMEF from HP L. by UV–vis

Methylene blue (MB) as a water-soluble dye, which has received much attention as an electroactive probe for the detection of DNA damage. In this experiment, ds-DNA damage caused by Fenton system was detected through UV–vis method using MB as indicator. The results were shown in Fig. 4 A, MB had a clear UV absorption peak at 590 nm (curve a). When a certain amount of MB solution was added to Fenton solution, the damage was sequentially detected for 0 min (curve b), 10 min (curve c), 20 min (curve d), 30 min (curve e), and 30 min (curve f), 30 min (curve e), and 40 min (curve f). A certain amount of damaged ds-DNA solution was taken for UV detection. The results showed that the absorbance value of MB decreased gradually after the addition of ds-DNA solution, which was probably due to the reaction between MB and ds-DNA, and the absorbance value decreased continuously with the increase of damage time. Curve (g) showed the UV spectra of ds-DNA solution treated with Fenton solution containing certain concentration of AA for 10 min, and the absorbance value increased. Compared with curve (c), the absorbance value increased, indicating that AA played a certain role in protecting ds-DNA oxidative damage. Curve (h) was the UV absorbance visible curve of ds-DNA mixed solution after 10 min treatment in Fenton solution containing certain concentration of G-S-1. It found that the absorbance value of MB was greater than that in the same conditions without G-S-1 (curve c). And curve (g) still has a larger absorbance compared with curve (h). Taken together, these results indicated that G-S-1 has a certain inhibitory effect on ds-DNA damage, but not as strong as AA. This experimental result is consistent with the results of the above electrochemical method to detect antioxidant activity.

Fig. 4 B was the change curve of the relative absorbance of MB (A_t/A_0) varies with the damage time of ds-DNA by Fenton system before and after adding AA and G-S-1 at the same concentration (0.90 mg/mL) to ds-DNA solution. As can be seen from the figure, when ds-DNA was only damaged in Fenton system (curve a), A_t/A_0 decreased at the fastest rate. When it contained a certain amount of AA (curve b) and G-S-1 (curve c), which decreased at a more gradual rate than curve a. This indicated that the addition of AA and G-S-1 significantly weakened the degree of ds-DNA damage. However, the rate of decrease of G-S-1 was significantly faster than that of AA, which indicated that AA has a stronger antioxidant capacity than G-S-1 and inhibited ds-DNA damage to a greater extent.

4. Conclusion

In this study, a ds-DNA/AuNPs/AC@CS/GCE electrochemical biosensor for evaluating the antioxidant activity of secondary metabolites of endophytic fungi (SMEF) from *Hypericum perforatum* L. (*HP* L.) was fabricated based on the AC@CS and AuNPs using the method of layer by layer assembly. The AuNPs with good biocompatibility provided a large effective surface area and strong adsorptive ability as the sensing interface, which could immobilize ds-DNA more efficiently, while the AC@CS with excellent electrical conductivity remarkably improved the sensitivity and accuracy of ds-DNA/AuNPs/AC@CS/GCE sensor. The experimental conditions affecting the evaluation results of the biosensor were optimized by square wave voltammetry (SWV) using $Ru(NH_3)_6^{3+}$ as the probe, and the antioxidant activity of various SMEF from *HP* L. was evaluated by the proposed biosensor. Meanwhile, the results of the biosensor were also verified by Ultraviolet and visible spectrophotometry (UV–vis). According to the optimized experimental results, the biosensors have a high levels of oxidative DNA damage at pH 6.0 and Fenton solution system with Fe^{2+} to OH^- ratio of 1:3 for 30 min.

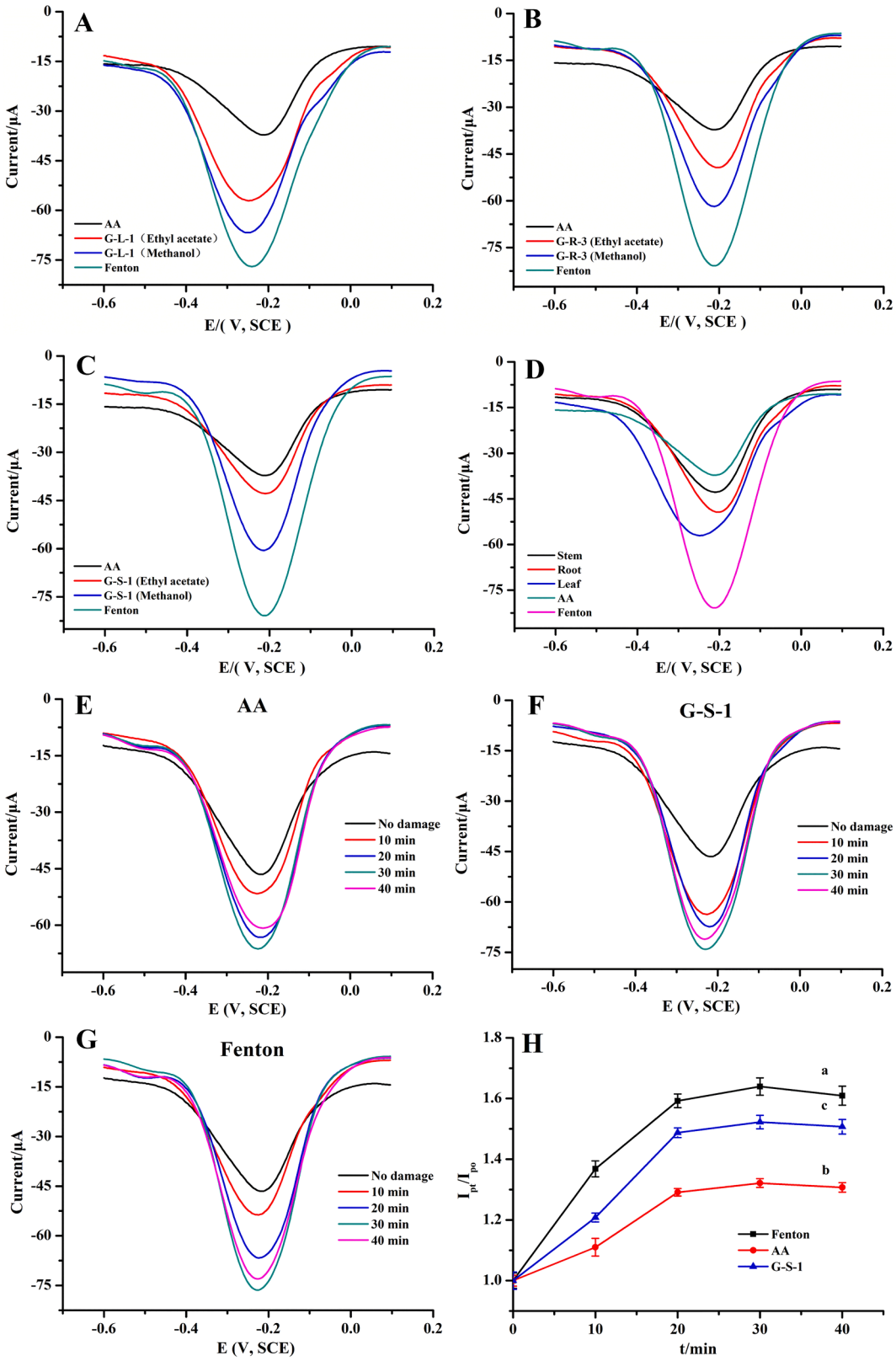

Fig. 3. The modified electrodes with $Ru(NH_3)_6^{3+}$ as the probe solution in the Fenton system containing (A) 0.90 mg/mL of AA, G-L-1 ethyl acetate, G-L-1 methanol and the Fenton system without antioxidant. (B) 0.90 mg/mL of AA, G-*R*-3 ethyl acetate, G-*R*-3 methanol and the Fenton system without antioxidant. (C) SWV detection signal of 30 min damage in Fenton system with 0.90 mg/mL AA, G-S-1 ethyl acetate, G-S-1 methanol and Fenton system without antioxidants. (D) Comparison of SWV signal of modified electrode after 30 min damage in Fenton system containing 0.90 mg/mL AA, G-S-1 ethyl acetate, G-*R*-3 ethyl acetate, G-L-1 ethyl acetate and antioxidant free. SWV detection signal after different time of injury in Fenton system containing (E) 0.90 mg/mL AA, (F) 0.90 mg/mL of G-S-1 and (G) no antioxidant. (H) The trend of I_{pt}/I_{p0} of SWV detection signal after different times of damage at the modified electrode in (a) without antioxidant, (b) with 0.90 mg/mL AA, (c) with 0.90 mg/mL G-S.

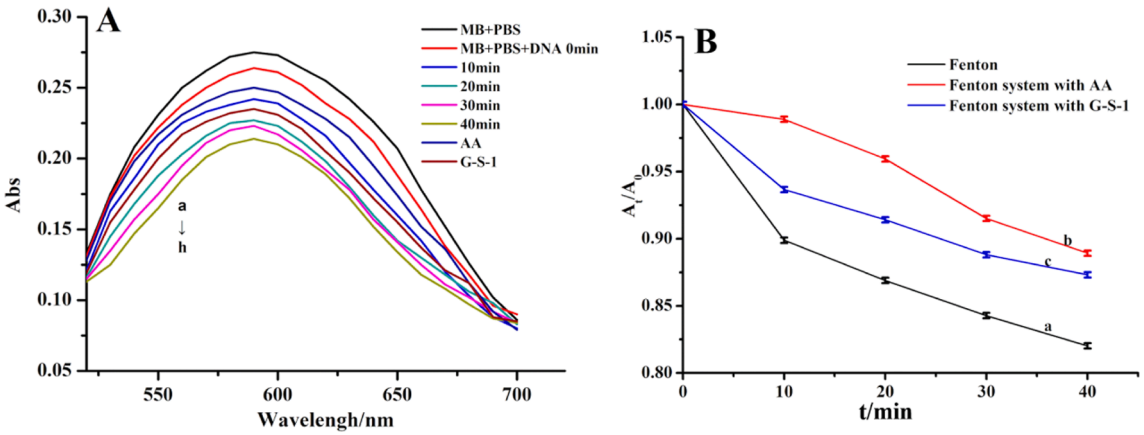

Fig. 4. (A) UV detection of ds-DNA treated in different solutions with MB as indicator (a) 20.00 μmol/L MB, 0.10 mol/L PBS (pH = 7.0), (b) 20.00 μmol/L MB, 0.10 mol/L PBS (pH = 7.0), 0.10 mg/mL Fenton solution treatment for 0 min, (c) 10 min, (d) 20 min, (e) 30 min, (f) 40 min of ds-DNA solution, (g) 20.00 μmol/L MB, 0.10 mol/L PBS (pH = 7.0), 0.10 mg/mL ds-DNA, 0.90 mg/mL AA damaged in Fenton system for 10 min, (h) 20.00 μmol/L MB, 0.10 mol/L PBS (pH = 7.0), 0.10 mg/mL ds-DNA, 0.90 mg/mL G-S-1 damaged in the Fenton system for 10 min. (B) MB as indicator for UV detection of ds-DNA after treatment in different solutions (a) Fenton system, (b) Fenton system containing a certain amount of AA, (c) Fenton system with a certain amount of G-S-1. And the trend of A_t/A_0 after 0 min, 10 min, 20 min, 30 min and 40 min of damage, respectively.

Among the crude extracts of SMEF from roots, stems and leaves of *HP* L., the crude extracts from stems presents a high antioxidant activity, but it is weaker than L-ascorbic acid. This result was consistent with the evaluation results of UV–vis spectrophotometric method, also the fabricated biosensor presents high stability and sensitivity. In a word, this study not only provides a convenient, efficient and promising platform for evaluation of the antioxidant activity of a wide variety of SMEF from *HP* L., but also provides a novel strategy for developing rapid screening and evaluation technique for the diverse activities of SMEF from medicinal plants.

Declaration of Competing Interest

The authors declare that they have no known competing financial interests or personal relationships that could have appeared to influence the work reported in this paper.

Data availability

Data will be made available on request.

Acknowledgments

The authors acknowledge the Natural Science Foundation of Gansu Province (No. 22JR5RA280); 2021 University Innovation Fund Project of Gansu Provincial Department of Education (No. 2021A-022); Gansu Province Youth Science and Technology Fund Project (No. 21JR7RA862); Lanzhou Science and Technology Plan Project (No. 2022-2-54); Gansu Province 2022 Drug Safety Supervision Research Project (No. 2022GSMPA0044); Wenzhou Municipal Science and Technology Plan Project (No. Y20220199); the 2020 PhD Research Start-up Fee of Lanzhou University of Technology and the 2022 Lanzhou University of Technology Innovation and Entrepreneurship Training Program for college students (No. DC2022579; DC2022584).

Appendix A. Supplementary material

Supplementary data to this article can be found online at https://doi.org/10.1016/j.bioelechem.2023.108400.

References

[1] M. Dziwenka, Chapter 40-St John's wort (*Hypericum perforatum* L.), Academic Press, 2021, pp. 661–695, doi: 10.1016/B978-0-12-821038-3.00040-9.
[2] K. Doukani, A.S.M. Selles, H. Bouhenni, Chapter 3.1.11-Hypericin and Pseudo Hypericin Occurring Chemicals Against Alzheimer's Disease, Academic Press, 2021, pp. 155–165, doi: 10.1016/B978-0-12-819212-2.00013-X.
[3] E. Özdemir, K. Alpınar, An ethnobotanical survey of medicinal plants in western part of central Taurus Mountains: Aladaglar (Nigde–Turkey), J. Ethnopharmacol. 166 (2015) 53–65, https://doi.org/10.1016/j.jep.2015.02.052.
[4] R. Méndez, M. Argüelles, G. Ballesteros, Flower, stem, and leaf extracts from *Hypericum perforatum* L. to synthesize gold anoparticles: effectiveness and antioxidant activity, Surf. Interf. (2022), 102181, https://doi.org/10.1016/j.surfin.2022.102181.
[5] N. Ramalhete, A. Machado, R. Serrano, E.T. Gomes, H. Mota-Filipe, O. Silva, Comparative study on the in vivo antidepressant activities of the Portuguese *Hypericum foliosum*, *Hypericum androsaemum* and *Hypericum perforatum* medicinal plants industrial, Crops Prod. 82 (2016) 29–36, https://doi.org/10.1016/j.indcrop.2015.12.014.
[6] S. Ergün, Gene regulation via miRNAs of *Hypericum perforatum* (St. John's wort) flower dietetically absorbed: an in silico approach to define potential biomarkers for prostate cancer, Comput. Biol. Chem. 80 (2019) 16–22, https://doi.org/10.1016/j.compbiolchem.2019.02.010.
[7] Z. Saddiqe, I. Naeem, A. Maimoona, A review of the antibacterial activity of *Hypericum perforatum* L, J. Ethnopharmacol. 131 (3) (2010) 511–552, https://doi.org/10.1016/j.jep.2010.07.034.
[8] Z. Hasan, H. Julistiono, N. Bermawie, I. Riyanti, R. Arifni, Soursop leaves (*Annona muricata* L.) endophytic fungi anticancer activity against HeLa cells, Saudi J. Biol. Sci. (2022), 103354, https://doi.org/10.1016/j.sjbs.2022.103354.
[9] H. Mohamed, A. Hassane, O. Atta, Y. Song, Deep learning strategies for active secondary metabolites biosynthesis from fungi: harnessing artificial manipulation and application, Biocatal. Agric. Biotechnol. 38 (2021), https://doi.org/10.1016/j.sjbs.2022.103354.
[10] H. Wu, Z. Yan, Y. Deng, et al., Endophytic fungi from the root tubers of medicinal plant *Stephania dielsiana* and their antimicrobial activity, Acta Ecol. Sin. 40 (5) (2020) 383–387, https://doi.org/10.1016/j.chnaes.2020.02.008.
[11] A.E.Z. Hasan, H. Julistiono, N. Bermawie, E. Riyanti, F.R. Arifni, Soursop leaves (*Annona muricata* L.) endophytic fungi anticancer activity against HeLa cells, Saudi J. Biol. Sci. 29(8) (2022) 103354, doi: 10.1016/j.sjbs.2022.103354.
[12] A. Kumar, K.L. Rana, D. Kour, T. Kaur, R. Devi, A.N. Yadav, N. Yadav, K. Singh, A. K. Saxena, 11-Endophytic fungi from medicinal plants: biodiversity and biotechnological applications, Microbial Endophytes (2020) 273–305, https://doi.org/10.1016/B978-0-12-819654-0.00011-9.
[13] N.T. Ujam, D.L. Ajaghaku, F.B.C. Okoye, C.O. Esimone, Antioxidant and immunosuppressive activities of extracts of endophytic fungi isolated from *Psidium guajava* and *Newbouldia laevis*, Phytomedicine 1 (2) (2021), https://doi.org/10.1016/j.phyplu.2021.100028.
[14] S.N. Orcajada, I. Conesa, A. Matencio, P.R. Bonilla, F.G. Carmona, J.M.L. Nicolás, The use of cyclodextrins as solubility enhancers in the ORAC method may cause interference in the measurement of antioxidant activity, Talanta 243 (2022), https://doi.org/10.1016/j.talanta.2022.123336.
[15] G. A, et al., Total antioxidant capacity as a tool to assess redox status: critical view and experimental data, Free Rad. Biol. Med. 29 (11) (2000) 1106–1114, doi: 10.1016/S0891-5849(00)00394-4.
[16] J. Yang, J. Chen, Y. Hao, Y. Liu, Identification of the DPPH radical scavenging reaction adducts of ferulic acid and sinapic acid and their structure-antioxidant

activity relationship, LWT 146 (2021), https://doi.org/10.1016/j.lwt.2021.111411.
[17] T.M.D. Santos, C. Martins, D.P. Bueno, I.J. Nunes, et al., Synthesis, molecular structure and antioxidant activity of bis [L (μ2-chloro) copper (II)] supported by phenoxy/naphthoxy–imine ligands, J. Inorg. Biochem. 210 (2020), https://doi.org/10.1016/j.jinorgbio.2020.111130.
[18] H. Fan, Y. Wu, T. Huang, N. Hong, H. Cui, G. Wei, F. Liao, J. Zhang, An electrochemical DNA sensor based on an integrated and automated DNA walker, Bioelectrochemistry 147 (2022), https://doi.org/10.1016/j.bioelechem.2022.108198.
[19] Y. Ye, X. Sun, Y. Zhang, X. Han, X. Sun, A novel cell-based electrochemical biosensor based on MnO2 catalysis for antioxidant activity evaluation of anthocyanins, Biosens. Bioelectron. 202 (2022), https://doi.org/10.1016/j.bios.2022.113990.
[20] F. Liu, X. Jiang, N. He, R. Yu, Z. Xue, X. Liu, Electrochemical investigation for enhancing cellular antioxidant defense system based on a superoxide anion sensor, Sens. Actuators B 368 (2022), https://doi.org/10.1016/j.snb.2022.132190.
[21] J. Dong, D. Zhang, C. Li, T. Bai, H. Jin, Z. Suo, A sensitive electrochemical sensor based on PtNPs@Cu-MOF signal probe and DNA walker signal amplification for Pb2+ detection, Bioelectrochemistry 146 (2022), https://doi.org/10.1016/j.bioelechem.2022.108134.
[22] A. Ensafi, N. Kazemnadi, M. Amini, B. Rezaei, Impedimetric DNA-biosensor for the study of dopamine induces DNA damage and investigation of inhibitory and repair effects of some antioxidants, Bioelectrochemistry 104 (2015) 71–78, https://doi.org/10.1016/j.bioelechem.2015.03.008.
[23] A. Şavk, H. Aydın, K. Cellat, F. Şen, A novel high performance non-enzymatic electrochemical glucose biosensor based on activated carbon-supported Pt-Ni nanocomposite, J. Mol. Liq. 300 (2020), https://doi.org/10.1016/j.molliq.2019.112355.
[24] A. Diouf, M. Moufid, D. Bouyahya, L. Österlund, N.E. Bari, B. Bouchikhi, An electrochemical sensor based on chitosan capped with gold nanoparticles combined with a voltammetric electronic tongue for quantitative aspirin detection in human physiological fluids and tablets, Mater. Sci. Eng.: C 110 (2020) 110665, doi: 10.1016/j.msec.2020.110665.
[25] K. Lota, I. Acznik, A. Sierczynska, G. Lota, The capacitance properties of activated carbon obtained from chitosan as the electrode material for electrochemical capacitors, Mater. Lett. 173 (2016) 72–75, https://doi.org/10.1016/j.matlet.2016.03.031.
[26] L. Wang, X. Wu, Y. Huang, X. Yang, Q. Wang, X. Chen, Improving the detection limit of Salmonella colorimetry using long ssDNA of asymmetric-PCR and non-functionalized AuNPs, Anal. Biochem. 626 (2021), https://doi.org/10.1016/j.ab.2021.114229.
[27] J. Tang, R. Huang, S. Zheng, S. Jiang, H. Yu, Z. Li, J. Wang, A sensitive and selective electrochemical sensor based on graphene quantum dots/gold nanoparticles nanocomposite modified electrode for the determination of luteolin in peanut hulls, Microchem. J. 145 (2019) 899–907, https://doi.org/10.1016/j.microc.2018.12.006.
[28] X. Wang, C. Jiao, Z. Yu, Electrochemical biosensor for assessment of the total antioxidant capacity of orange juice beverage based on the immobilizing DNA on a poly l-glutamic acid doped silver hybridized membrane, Sens. Actuators B 192 (2014) 628–633, https://doi.org/10.1016/j.snb.2013.11.025.
[29] M. Deng, L. Tao, Y. Qiao, W. Sun, S. Xie, Z. Shi, C. Qi, Y. Zhang, New cytotoxic secondary metabolites against human pancreatic cancer cells from the *Hypericum perforatum* endophytic fungus *Aspergillus terreus*, Fitoterapia 146 (2020), https://doi.org/10.1016/j.fitote.2020.104685.
[30] M. Pradeep, G. Franklin, Understanding the hypericin biosynthesis via reversible inhibition of dark gland development in *Hypericum perforatum* L, Ind. Crop. Prod. doi: 10.1016/j.indcrop.2015.12.014.
[31] R. Mustafa, R. Sukor, S. Eissa, A.N. Shahrom, N. Saari, S.M. Nor, Sensitive detection of mitragynine from *Mitragyna speciosa* Korth using an electrochemical immunosensor based on multiwalled carbon nanotubes/chitosan-modified carbon electrode, Sens. Actuators B 345 (2021), https://doi.org/10.1016/j.snb.2021.130356.
[32] H. Kaya, N. Haghmoradi, B. Yarar Kaplan, F. Kuralay, Platinum nanoparticles loaded carbon black: reduced graphene oxide hybrid platforms for label-free electrochemical DNA and oxidative DNA damage sensing, J. Electroanal. Chem. 910 (2022), https://doi.org/10.1016/j.jelechem.2022.116180.
[33] N. Nikzad, H. Parastar, Evaluation of the effect of organic pollutants exposure on the antioxidant activity, total phenolic and total flavonoid content of lettuce (*Lactuca sativa* L.) using UV–Vis spectrophotometry and chemometrics, Microchem. J. 170 (2021) 106632, doi: 10.1016/j.microc.2021.106632.
[34] W. Xu, T. Jin, Y. Dai, C. Liu, Surpassing the detection limit and accuracy of the electrochemical DNA sensor through the application of CRISPR Cas systems, Biosens. Bioelectron. 155 (2020), https://doi.org/10.1016/j.bios.2020.112100.